Synthesis and characterization of magnetic nanoparticles coated with silica through a sol-gel approach

(Síntese e caracterização de nanopartículas magnéticas revestidas com sílica através de um processo sol-gel)

A. L. Andrade, D. M. Souza, M. C. Pereira, J. D. Fabris, R. Z. Domingues
Departamento de Química, Universidade Federal de Minas Gerais, C.P. 702, Belo Horizonte, MG, 31270-901
rosanazd@ufmg.br

Abstract

This paper investigates the influence of reaction medium pH on silica-coating of magnetite nanoparticles. Magnetite nanoparticles were prepared by means of a reduction-precipitation method using ferric chloride as a starting material, which was partially reduced to ferrous salts by Na_2SO_3 before alkalinizing with ammonia. The particles were coated by sol-gel method with either ammonia or HCl aqueous solutions for either base- or acid-catalyzed hydrolysis, respectively. Powder X-ray diffraction, Fourier-transform infrared, and Zeta Potential were used for the characterization of oxides and of the coated magnetic nanoparticles. The observed difference of pH_{IEP} in KCl solution for pure silica (2.0), magnetite (5.0), and silica-coated magnetite (2.3) samples confirms that the coating process was effective since the charge surface properties of coated magnetic nanoparticles are close to that of pure silica, even though the Fourier-transform infrared spectra did not evidence the formation of Fe-O-Si bonds.
Keywords: magnetite, coating, nanoparticles.

Resumo

Este trabalho aborda a influência do pH do meio de reação, no procedimento de revestimento de nanopartículas magnéticas de magnetita, preparadas por redução-precipitação de cloreto férrico. O material de partida foi parcialmente reduzido a sal ferroso, por reação com Na_2SO_3*, antes da alcalinização, com amônia. As partículas foram revestidas, pelo método sol-gel, a partir de solução aquosa de amônia ou ácido clorídrico, para promover a hidrólise catalisada por base ou ácido, respectivamente. Os materiais, de óxidos de ferro e de nanopartículas magnéticas revestidas, assim produzidos, foram caracterizados por difração de raios X, método do pó, por infravermelho com transformada de Fourier e por potencial zeta para a determinação do pH do ponto isoelétrico (*pH_{IEP}*). A diferença observada do* pH_{IEP} *em solução de KCl para amostras de sílica pura (2,0), magnetita (5,0) e para a magnetita revestida por sílica (2,3) confirma que o processo de revestimento foi efetivo, uma vez que as propriedades de carga de superfície das nanopartículas magnéticas revestidas são próximas às da sílica pura, apesar de o espectro de infravermelho com transformada de Fourier não evidenciar padrões espectrais característicos de ligações Fe-O-Si.*
Palavras-chave: *magnetita, revestimento, nanopartículas.*

INTRODUCTION

Chemically synthesized magnetic nanoparticles have drawn much attention [1-3] due to the unique magnetic properties associated to their size magnitude and distribution uniformity. Among these particles, magnetite nanoparticles have been widely studied with biomedical applications in view, such as magnetic resonance imaging for clinical diagnosis, magnetic drug targeting, hyperthermia anti-cancer strategy, and enzyme immobilization [4-11].

Magnetite (Fe_3O_4), a common magnetic iron oxide, has a cubic inverse spinel structure with oxygen forming a FCC closed packing and Fe cations occupying the interstitial tetrahedral and octahedral sites [12]. The electrons can hop between Fe^{2+} and Fe^{3+} ions in octahedral sites even at room temperature, rendering magnetite an important half-metallic material [13]. Due to the anisotropic dipolar attraction, unmodified magnetic nanoparticles of iron oxides tend to aggregate into large clusters and thus lose the specific properties associated with single-domain. In addition, the reactivity of iron oxide particles has been shown to increase greatly as their dimensions are reduced and they may undergo rapid biodegradation when exposed directly to biological systems [14, 15]. Suitable coating is essential to prevent such limitation [16]. Silica coating of magnetic nanoparticles has become a promising and important approach in the development of magnetic nanoparticles for both fundamental study and technological research. The formation of a silica coating on the surface of iron oxide nanoparticles could help prevent their aggregation in liquid and improve their chemical stability. Another advantage of silica-coating iron oxide nanoparticles is that the silanol-terminated surface groups may be modified with various coupling agents to covalently bind to specific ligands

[17-19]. Finally, the most important is that the silica layer provides magnetic nanoparticles with a surface chemically friendly to biological systems.

Among various chemical synthesis coating methods, the sol-gel process offers several advantages, including good homogeneity, low cost, and high purity.

The electrical nature of the sample-water interface is the result of the hydrolysis of the surface species followed by pH-dependent dissociation of surface hydroxyls. A characteristic property of the sample surface is the condition of surface zero charge, known as zero point of charge (zpc), which is usually determined by some form of acid–base titration technique. Surface characteristics may also be investigated by electrokinetic phenomena, which involve the inter-relation between mechanical and electrical effects at a moving interface. Electrokinetic results are generally expressed in terms of zeta potential, which may be calculated from the electrophoretic mobility of particles through a field with known strength. The term, isoelectric point (iep) refers to conditions under which the zeta potential is zero. The surface potential need not be zero when the zeta potential is zero, particularly in the case of specifically adsorbed ions, hence the zpc and iep need not be the same [20].

In this work, zeta-potential measurements are used to monitor coating efficiency besides its characterization by X-ray diffraction (XRD), and Fourier-transform infrared spectroscopy.

EXPERIMENTAL

Materials

Reagent grade $FeCl_3{\cdot}6H_2O$ and Na_2SO_3, ammonium hydroxide, ethyl alcohol, acetone, chloridric acid (Synth), and tetraethyl orthosilicate (TEOS -Aldrich 98%) were used as purchased.

Iron oxide nanoparticle synthesis

The method proposed in [21] was used in the preparation of nanoparticulate magnetite. Magnetic particles were synthesized using 15 mL $FeCl_3.6H_2O$ (2 $mol.L^{-1}$) dissolved in 0.25 $mol.L^{-1}$ HCl, 10 mL of Na_2SO_3 stock solution (1 $mol.L^{-1}$), and 25.4 mL of ammonium hydroxide solution diluted to a total volume of 400 mL. The reaction was carried out in 1000-mL 3-necked round bottom flask by bubbling a protective gas (nitrogen) for ensure an inert atmosphere. Just after mixing Fe^{3+} and SO_3^{2-}, the color of the solution changed from light yellow to red and afterwards back to yellow. At that moment, the diluted ammonia solution was poured into the solution quickly under vigorous stirring and a black precipitate was formed. The reaction was continued by stirring for an additional 30 min. The supernatant was discarded and the black precipitate was centrifuged with distilled water. This procedure was repeated five times and then, the precipitate obtained was centrifuged with acetone and subsequently placed in a desiccator and dried at room temperature. Then, the sample was reduced in a Pyrex tube under H_2 flowing at 50 $mL.min^{-1}$ for 2 h at increasing temperature from 20 to 250 ºC at a rate of 10 $ºC.min^{-1}$ which was held for a total heating period of 2 h. This sample was labeled Mt.

Silica-coating of iron oxide nanoparticle

Silica coating was carried out using modified reported methods [22, 23]. Deng e cols. prepared silica-coated magnetite nanoparticles using different types of alcohols, and various volume ratios of ethanol to water ($V_{E/W}$). The feeding amount of catalyst and TEOS were also varied and the synthesis products were carefully characterized. In our study we used the optimized experimental conditions obtained in those studies. The formulations of each reaction were the same except for the type of catalyst. Typically 0.04 g of magnetic powder was diluted with 160 mL ethyl alcohol. This dispersion was homogenized by ultrasonic vibration in water bath for 10 min. Finally, 40 mL water, 1 mL TEOS, and either 5 mL ammonia aqueous (pH 10) or 5 mL of acidified (HCl - pH 1.7) aqueous solution were slowly added to this dispersion and stirred for 24 h. At this point, magnetic separation was made with the help of a permanent magnet and the magnetic powder collected alone was thoroughly washed with distilled water six times. These samples were named MtSi-a and MtSi-b, where a and b denote the acid (pH equal 4.1) and basic media (pH equal 11.4), respectively. The samples were placed under humidified atmosphere overnight and next treated in dry room atmosphere for 96 h.

Glass synthesis

A silica glass control sample was prepared for zeta potential study. In this case TEOS was added to an acidified (HCl - pH 1.7) aqueous solution, and next added to ethanol in a molar proportion of H_2O:TEOS:CH_3CH_2OH of 4:1:4. The solution was magnetically stirred until gelation. The material was placed under humidified atmosphere overnight and next treated in dry atmosphere for 24 h.

Characterization methods

Sample structure, homogeneity, and the formation of silica-coated magnetite nanoparticles were evaluated by comparison of FTIR spectra of coated and non-coated samples. For these analyses, samples were compacted with KBr (approximately 1%) and analyzed in transmission mode in a Perkin Elmer Spectrum GX spectrophotometer. X-ray diffraction measurements were performed in a Rigaku model Geigerflex apparatus using Cukα radiation from 20 to 80º (2θ) at a scan rate of $4º.min^{-1}$ and silicon as an external standard.

Zeta Potential (ξ) and particle size were determined in a Nano Size ZS apparatus. For zeta potential measurements the ground material was suspended in water and homogenized with ultrasound for 15 min. After this time, another suspension was made by adding drops of the previous suspension to an aqueous solution of KCL 10^{-3} mol.L^{-1}. The pH of this solution was measured and adjusted with either aqueous NaOH 10^{-3} mol.L^{-1} or HNO_3 10^{-3} mol.L^{-1}. ξ was measured as a pH function. For particle size measurements, an aqueous suspension of magnetic powders were ultrasonic for 10 min and next they are left to rest during 30 min.

RESULTS

Magnetite nanoparticles

XRD results (Fig. 1a) showed the presence of two phases corresponding to magnetite and elementary iron in sample Mt. The line broadening observed is essentially due to the nanoparticle size effect. The average particle size of this magnetite sample estimated from breadths of reflection 311 in Scherrer equation was 10 nm.

Fig. 2b shows the FTIR spectra of sample Mt. Since magnetite has an inverse spinel-type structure, it shows bands indicating the vibrations M_T–O–M_O ($\nu_1 \approx 600$–550 cm^{-1}), M_O–O ($\nu_2 \approx 470$ cm^{-1}), and M_T–M_O ($\nu_3 \approx 350$–400 cm^{-1}), where M_T and M_O correspond to the metal occupying tetrahedral and octahedral positions, respectively [24-26]. Due to instrument limitations, we were unable to observe vibrations type 'ν_3', although 'ν_1'- and 'ν_2'-type bands were well defined. Table I shows the reported absorbance values of various iron oxides [27, 28].

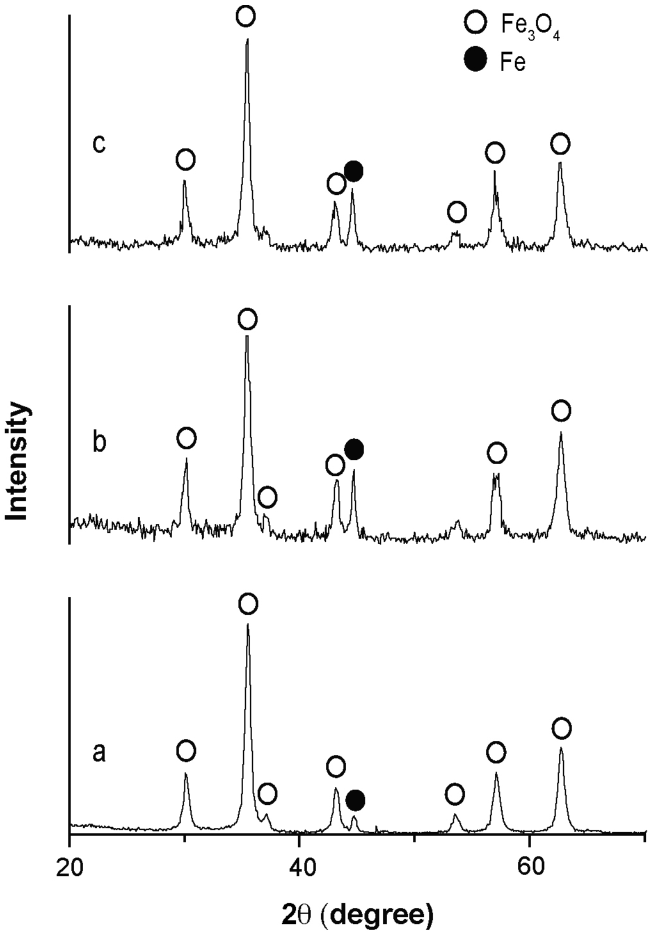

Figure 1: X-ray diffraction patterns of samples: (a) Mt, (b) MtSi-b, and (c) MtSi-a.

[Figura 1: Difratogramas de raios X das amostras Mt (a), MtSi-b (b) e MtSi-a (c).]

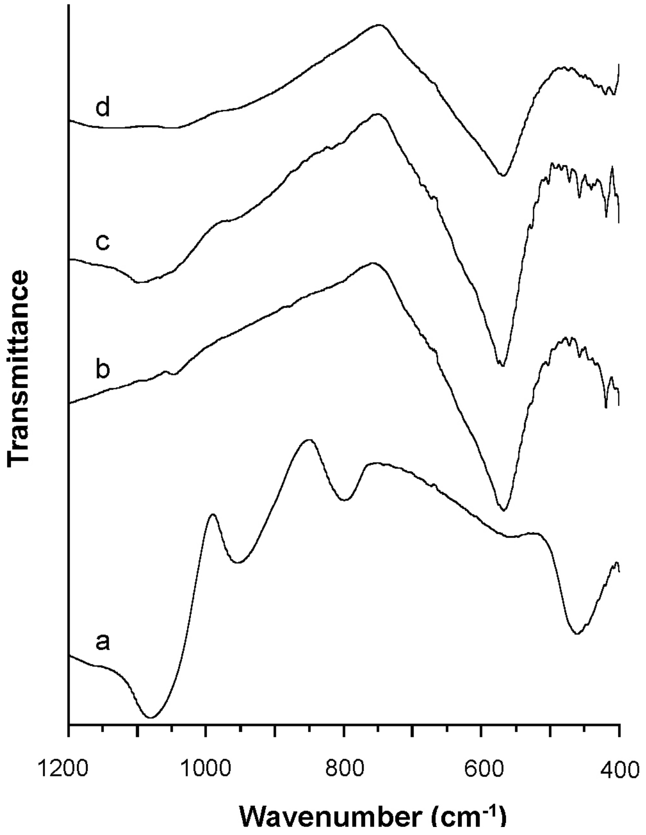

Figure 2: FTIR spectra of (a) glass, (b) Mt, (c) MtSi-b, and (d) MtSi-a.

[Figura 2: Espectro infra-vermelho com transformada de Fourier do vidro (a), Mt (b), MtSi-b (c) e MtSi-a (d).]

Fig. 3 shows the variation of the zeta potential as a function of pH solution for sample Mt. The pH corresponding to the isoelectric point (pH_{IEP}) of this sample is about 5.0.

Table I - IR bands of various iron oxides.

[Tabela I - Bandas da região do infra-vermelho de vários óxidos de ferro.]

Iron oxide	IR bands (cm^{-1})
Magnetite	590
Maghemite	630, 590, 570, 450
Hematite	540, 470
Feroxyhyte	1110, 920, 790, 670
Lepidocrocite	1026, 1161, 753
Goethite	890, 797
Akaganeite	840, 640

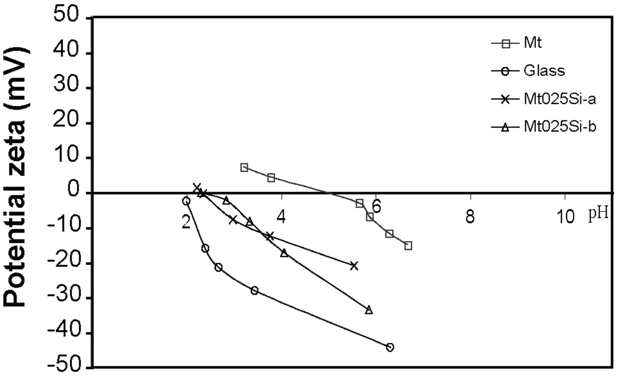

Figure 3: Variation of zeta potential of glass, Mt, MtSi-b, and MtSi-a with pH.

[Figura 3: Potencial zeta de vidro, Mt, MtSi-b e MtSi-a em função do pH.]

These results are in a good agreement with data found in the literature [29].

Silica-coated magnetite particles

Fig. 1b and c shows the X-ray diffraction patterns of silica-coated samples. The spectrum includes Fe_3O_4 and some Fe diffraction peaks, and it is very similar to that of non-coated sample as expected.

FTIR spectrum of silica glass control sample (Fig 2a) presented bands at 1080, 800, and 460 cm^{-1} due to the Si-O-Si bonds [30-32] and a peak at 960 cm^{-1} associated to Si-OH bond vibrations [33]. Sample MtSi-b (Fig. 2c) presented peaks related to the Si-O-Si bond at 1080 cm^{-1} and 800 cm^{-1}, besides a peak at 575 cm^{-1} associated with Fe-O bonds. The shoulder at 960 cm^{-1} present in the FTIR spectrum of this sample is composed of contributions from Si-O-H stretching and Fe-O vibrations [34]. As no substantial shifts are observed when coated and non-coated spectra are compared, the formation of Fe-O-Si bonds may not be evoked.

The FTIR spectrum of sample MtSi-a (Fig. 2d) showed a broad band characteristic of Si-O bands at about 1200 to 900 cm^{-1} and another at 570 cm^{-1}, characteristic of magnetite.

Fig. 3 shows the variation of the zeta potential as a function of solution pH for samples Mt, MtSi-a, MtSi-b, and for pure silica glass. The pH corresponding to the isoelectric point (pH_{IEP}) of the Mt sample is about 5.0. Samples MtSi-a and MtSi-b presented a pH_{IEP} of 2.3, and the pH_{IEP} of pure glass is about 2.0.

DISCUSSION

To verify the surface charge effect of magnetite particles, the zeta potential of silica-coated and non-coated particles was measured as a function of the solution pH (Fig. 3). The pH_{iep} of magnetite nanoparticles is about 5.0, while all coated particles showed a pH dependency similar to that of pure silica. Their pH_{IEP} was about 2.3, whilst pure silica has a pH_{IEP} equal to 2.0. The observed difference of pH_{IEP} in KCl solution confirms that the coating process was effective since the charge surface properties of magnetic nanoparticles are close to that of pure silica. The nature of the species present in the base and acid catalyst medium coating should be different. Magnetite powders have a pH_{iep} equal to 5.0, which means that for coating at pH 11.4, the magnetite presented a negative surface, while that coated at pH 4.1 presented a positive surface. It is expected that at pH 11.4 FeO^- groups predominate over $FeOH^+_2$ groups on magnetite surface in contrast to that at pH 4.1. However, our results show that coating occurred in both conditions.

Hypotheses of specific interactions between magnetite nanoparticles and silica have been advanced in the literature. Particle dispersability in the silica matrices may result from various types of interactions: covalent, through Si-0-Fe bond formation; electrostatic, between negatively charged Si-0 terminal ligands and positively charged groups on the particle surface; or hydrogen-bond interactions between hydration layers of silanol groups and the particle surface [35]. Bruni *et al.* [36] proposed a model for Fe_2O_3-SiO_2 nanocomposites in which iron oxide nanocrystals in silica matrix pores are closer to the matrix surface with the elimination of interconnected water by producing a magnetic interaction between iron (III) and silica ions. The presence of Si-O-Fe bonds in the dried gel strongly indicates an interaction between well isolated Fe^{3+} ions and the nearest silica matrix. Li *et al.* [37] observed similar results for $NiFe_2O_4$ nanocrystals dispersed in a silica matrix. IR and EPR spectroscopies were used in those studies to follow the changes. In our study, no extra bands related to Fe-O-Si bonds appeared in Fourier-transform infrared spectra of coated samples. Therefore, if Fe^{+3} – Si interaction occurs, it seems to be very faint. In fact, the Bruni model [36] suggests that the Fe_3O_4 nanoparticles interact with either the silica matrix or the silanol groups on the surface of the cavities where they are formed. After heating at 300, 500, and 700 °C, the vibration bands due to adsorbed H_2O molecules and silanol groups were little intense as polycondensation takes place. The Fe-O-Si band (590 cm^{-1}) appears after heating at 700 °C.

CONCLUSION

Zeta potential measurements showed that magnetite nanoparticles were successfully coated with silica in base- and acid-catalysis synthesis conditions. In both cases, coated magnetite presented almost the same pH_{IEP} as that of the pure glass sample. Moreover, the nanoparticles remained magnetic after coating and their particle size decreased about 30% after coating, probably due to the expected effect of the silica coating preventing nanoparticle agglomeration.

ACKNOWLEDGMENTS

The authors acknowledge financial support provided by FAPEMIG.

REFERENCES

[1] S. Sun, C. B. Murry, D. Welle, L. Folk, A. Moser, Science **287** (2002) 1989.
[2] M. Chen, D. E. Nikles, Nano Lett. **2** (2002) 211.
[3] E. V. Shevchenko, D. V. Talapin, A. L. Rogach, A. Kornowski, M. Haase, H. Weller, J. Am. Chem. Soc. **124** (2002) 11480.
[4] D. K. Kim, Y. Zhang, J. Kehr, T. Klason, B. Bjelke, M. Muhammed, J. Magn. Magn. Mater. **225** (2001) 256.
[5] C. H. Reynolds, N. Annan, K. Beshah, J. H. Huber, S. H. Shaber, R. E. Lenkinski, J. A. Wortman, J. Am. Chem. Soc. **122** (2000) 8940.
[6] A. S. Lubbe, C. Bergemann, H. Riess, F. Schriever, P. Reichardt, K. Possinger, M. Matthias, B. Dorken, F. Herrmann, R. Gurtler, P. Hohenberger, N. Haas, R. Sohr, B. Sander, A. J. Lemke, D. Ohlendorf, W. Huhnt, D. Huhn, Cancer Res. **56** (1996) 4686.
[7] C. Bergemann, D. Muller-Schulte, J. Oster, L. Brassard, A. S. Lubbe, J. Magn. Magn. Mater, **194** (1999) 45.
[8] D. C. F. Chan, D. B. Kirpotin, P. A. Bunn, J. Magn. Magn. Mater. **122** (1993) 374.
[9] A. Jordan, R. Scholz, P. Wust, H. Schirra, T. Schiestel, H. Schmidt, R. Felix, J. Magn. Magn. Mater. **194** (1999) 185.
[10] A. Dyal, K. Loos, M. Noto, S. W. Chang, C. Spagnoli, K. V. P. M. Shafi, A. Ulman, M. Cowman, R. A. Gross, J. Am. Chem. Soc. **125** (2003) 1684.
[11] M. Wakamatsu, N. Takeuchi, S. Ishida, Rep. Asahi Glass Found. **56** (1990) 243.
[12] R. M. Cornell, U. Schwertmann, The Iron Oxides: Structure, Properties, Reactions, Occurrence and Uses, VCH, New York, USA (1996) pp. 28–29.
[13] E. J. W. Verwey, Nature **144** (1939) 327.
[14] S. Santra, R. Tapec, N. Theodoropoulou, J. Dobson, A. Hebard, W. H. Tan, Langmuir **17** (2001) 2900.
[15] H. H. Yang, S. Q. Zhang, X. L. Chen, Z. X. Zhuang, J. G. Xu, X. R. Wang, Anal. Chem. **76** (2004) 1316.
[16] Z. Ma, Y. Guan, H. Liu, J. Magn. Magn. Mater. **301** (2006) 469.
[17] A. P. Philipse, M. P. B. van Bruggen, C. Pathmamanoharan, Langmuir **10** (1994) 92.
[18] Q. Liu, Z. Xu, J. A. Finch, R. Egerton, Chem. Mater. **10** (1998) 3936.
[19] X. Q. Liu, Z. Y. Ma, J. M. Xing, H. Z. Liu, J. Magn. Magn. Mater. **270** (2004) 1.
[20] K. Quast, Miner. Eng. **19** (2006) 582.
[21] S. C. Qu, H. B. Yang, D. W. Ren, S. H. Kan, G. T. Zou, D. M. Li, M. H. Li, J. Colloid Interface Sci. **215** (1999) 190.
[22] Y. H. Deng, C. C. Wang, J. H. Hu, W. L. Yang, S. K. Fu, Colloids Surf. A, Physicochem. Eng. Asp. **262** (2005) 87.
[23] W. Stober, A. Fink, E. Bohn, J. Colloid Interface Sci. **26** (1968) 62.
[24] E. Barrado, F. Prieto, J. Medina, F. A. López, J. Alloys Compd. **335** (2002) 203.
[25] J. L. M. de Vidales, A. López-Delgado, E. Vila, F. A. López, J. Alloys Compd. **287** (1999) 276.
[26] M. Ma, Y. Zhang, W. Yu, H. Y. Shen, H. Q. Zhang, N. Gu, Colloids Surf. A, Physicochem. Eng. Asp. **212** (2003) 219.
[27] R. M. Cornell, The Iron Oxides: Structure, Properties, Reactions, Occurrences and Uses, Wiley, New York, USA, ISBN 3527302743 (2003).
[28] U. Schwertzman, R. M. Cornell, Iron Oxides in the Laboratory-Preparation and Characterization, VCH Verlagsgesellschaft, Weiden, Germany (1991).
[29] M. Erdemoglu, M. Sarıkaya, J. Colloid Interface Sci. **300** (2006) 795.
[30] A. Bertoluzza, C. Fagnano, M. A. Morelli, V. Gottardi, M. Guglielni, J. Non-Cryst. Solids **48** (1982) 117.
[31] M. C. Matos, L. M. Ilharco, R. M. Almeida, J. Non-Cryst. Solids **147** (1992) 232.
[32] P. Y. Chu, D. E. Clark, Spectrosc. Lett. **25** (1992) 201.
[33] H. Yoshino, K. Kamiya, H. Nasu, J. Non-Cryst. Solids **126** (1990) 68.
[34] A. Al-bawabe, S.E. Friberg, J. Sjoblom, G. Farrington, J. Disper. Sci. Technol. **19** (1998) 613.
[35] C. Chaneac, E. Tronc, J. P. Jolivet, J. Mater. Chem. **6** (1996) 1905.
[36] S. Bruni, F. Cariati, M. Casu, A. Lai, A. Musinu, G. Piccaluga, S. Solinas, Nanostruct. Mater. **11** (1999) 573.
[37] G. S. Li, L. P. Li, R. L. Smith, H. Inomata, J. Mol. Struct. **560** (2001) 87.

(Rec. 12/12/2008, Ac. 13/02/2009)